Available online at www.sciencedirect.com

SciVerse ScienceDirect

Geochimica et Cosmochimica Acta 109 (2013) 306–311

Geochimica et Cosmochimica Acta

www.elsevier.com/locate/gca

Oxygen isotope partitioning between immiscible silicate melts with H_2O, P and S

Gregory W. Lester *, T.K. Kyser, Alan H. Clark

Queens University, Department of Geological Sciences and Geological Engineering, Canada

Received 19 March 2012; accepted in revised form 27 January 2013; available online 16 February 2013

Abstract

Differences between the $\delta^{18}O$ values of immiscible Si- and Fe-rich melts in the systems Fe_2SiO_4–Fe_3O_4–$KAlSi_2O_6$–SiO_2, Fe_3O_4–$KAlSi_2O_6$–SiO_2, and Fe_3O_4–Fe_2O_3–$KAlSi_2O_6$–SiO_2, with H_2O, H_2O + P or H_2O + S have been determined in isothermal, isobaric experiments at 1100 and 1200 °C and 200 MPa. The $\Delta^{18}O$ values for conjugate Fe_2SiO_4–Fe_3O_4–$KAlSi_2O_6$–SiO_2 + H_2O and, Fe_3O_4–$KAlSi_2O_6$–SiO_2·$KAlSi_2O_6$–SiO_2 + H_2O melts are only 0.4–0.6‰ and do not differ significantly from those for anhydrous melts of similar composition. The $\Delta^{18}O$ values for melts with added H_2O + P or S are more variable, ranging from 0.0 to 0.8‰. Partitioning of ^{18}O between the immiscible melts is 0.6–1‰ less than the partitioning reported for melt–mineral and mineral–mineral pairs. The partitioning of ^{18}O in the network modifier-bearing immiscible melts is not controlled by the relative degree of polymerization in the melts or fO_2. The upper limit of the range of $\Delta^{18}O$ values (<1‰), and the variation in the $\delta^{18}O$ values of conjugate melts that occurs with the inclusion of network modifying constituents, suggest that in some cases, oxygen isotope ratios might be useful to distinguish lithologies evolved from coexisting immiscible silicate melts, from lithologies that have evolved by crystal fractionation only.

1. INTRODUCTION

Revived interest in the petrogenetic role of silicate immiscibility has called attention to the need to constrain further the chemical and physical characteristics of two-liquid systems, particularly the effects of *P–T–X* parameters on partitioning between conjugate liquids (Veksler et al., 2006; Philpotts, 2008). The fractionation of oxygen isotopes between phases in natural silicate liquids is normally small, generally less than 1‰ (Taylor and Sheppard, 1986; Kyser 1990). However, processes involving phases with distinct chemical or physical properties, such as CO_2 degassing (Pineau et al., 1976) or fractional crystallization (Taylor and Epstein, 1962), can affect the isotopic composition of silicate liquids. Kyser et al. (1998) determined experimentally that differences in the crystallochemical properties of Si- and Fe-rich immiscible liquids in the system Fe_2SiO_4–$KAlSi_2O_6$–SiO_2 at 1180 °C and 0.1 MPa were sufficient to induce oxygen isotope fractionation between conjugate immiscible melts, the Si-rich liquids having $\delta^{18}O$ values 0.5–0.6‰ higher than those of the Fe-rich liquids.

Major and trace element partitioning between immiscible silicate liquids is similarly controlled by differences in the crystallochemical properties of the conjugate melts, in particular the ratio of network-modifying to network -forming components in the melts (Watson, 1976; Vicenzi et al., 1994; Bogaerts and Schmidt, 2006).The effects of $H_2O \pm P$ or S and fO_2 on silicate immiscibility (Lester, 2012) indicate that the addition of these components or variations in fO_2 in the system Fe_2SiO_4–Fe_3O_4–$KAlSi_2O_6$–SiO_2 (fayalite–magnetite–leucite–quartz), Fe_3O_4–$KAlSi_2O_6$–SiO_2 (magnetite–leucite–quartz) and Fe_3O_4–Fe_2O_3–$KAlSi_2O_6$–SiO_2 (magnetite–hematite–leucite–quartz) influence the crystallochemical properties of conjugate immiscible liquids, suppressing system liquids temperatures, broadening the miscibility gap, thus increasing the degree

* Corresponding author.
E-mail addresses: glesfo2@yahoo.com (G.W. Lester), kyser@geol.queensu.ca (T.K. Kyser).

0016-7037/$ - see front matter © 2013 Elsevier Ltd. All rights reserved.
http://dx.doi.org/10.1016/j.gca.2013.01.037

of partitioning of most major and trace elements between immiscible Fe- and Si-rich melts. In theory, the demonstrated changes to the crystallochemical properties of the immiscible liquids could similarly produce changes to the oxygen isotope proportioning between the immiscible melts.

This study assesses the magnitude of oxygen isotope fractionation between Fe- and Si-rich conjugate melts incorporating $H_2O \pm P$ or S, and with variation in fO_2, in the systems Fa–Lc–Qtz and Mt–Lc–Qtz. Oxygen isotope fractionation in the systems Fa–Lc–Qtz–H_2O and Mt–Lc–Qtz–H_2O is consistent with that observed in the anhydrous system regardless of fO_2. In the systems Fa–Lc–Qtz–H_2O and Mt–Lc–Qtz–H_2O with P or S, there are small, but significant differences in $\Delta^{18}O$ ($\delta^{18}O_{sil\text{-}liquid} - \delta^{18}O_{Fe\text{-}liquid}$) values relative to those observed in the anhydrous (Kyser et al., 1998), or H_2O-only systems (this study), suggesting that the inclusion of P or S in silicate melts can cause sufficient change in the crystallochemical properties of the melts to influence the partitioning of oxygen isotopes.

2. EXPERIMENTAL PROCEDURE

The effect of immiscibility on oxygen isotope ratios in silicate melts with H_2O, P or S was examined using a base-composition plotting on the 30 wt% FeO isopleth in the system Fe_2SiO_4–$KAlSi_2O6$–SiO_2 (Fa–Lc–Qtz) incorporating 10 wt% H_2O (total wt. solids) and molar equivalent quantities of either P or S (2.06 wt% P or 2.14 wt% S, i.e. 6.66×10^{-4} mol/g major element constituents) at 1100 and 1200 °C and 200 MPa (Fig. 1). Experimental charges were prepared from mixtures of SiO_2 (cristobalite), Al_2O_3, $K_2Si_2O_5$, FeO, Fe_2O_3, and Fe_2P or FeS (Table 1).

To minimize the fO_2 gradient between melts and external solid buffers, $Fe^{3+}/\Sigma Fe$ values for the melts synthesized in this study were estimated by the method of Schuessler et al. (2008) at $T = 1200$ °C, fO_2 of quartz–fayalite–magnetite (QFM), nickel–nickel oxide (NNO) or magnetite–hematite (MH) buffers at 200 MPa pressure. The $FeO_{(total)}$ component of each base-mixture comprises FeO and Fe_2O_3, or FeO, Fe_2O_3 and Fe_2P or FeS in proportions that approximate the $Fe^{3+}/\Sigma Fe$ values calculated for the selected experimental conditions.

Oxygen fugacity in the experimental capsules was regulated using the conventional double-capsule, metal–metal oxide + water configuration (Chou and Cygan, 1990).

Experimental capsules were prepared by loading the desired quantity of starting material, or starting material + H_2O, into a 2 mm (outside diameter) platinum capsule. Experimental capsules were loaded into a 5 mm (outside diameter) platinum capsule containing H_2O and one of the selected solid-oxide oxygen buffers, QFM, NNO or MH. Both inner experimental capsules and outer buffer-bearing capsules were sealed by welding.

Experiments were carried out in Kanthal™ or platinum-wound furnaces placed in an internally-heated pressure vessel under isobaric conditions (200, ±10 MPa), isothermally at 1100 or 1200 °C for two hours using argon as the pressure medium. The pressure vessel, similar in design to that described by Holloway (1971), was modified to allow the vessel to rotate from the horizontal run position to a vertical quench position. Rapid isobaric cooling of the experimental capsules was achieved as the vessel was rotated towards the vertical, causing the capsule to drop from the hot spot to the unheated, water-cooled end of the pressure chamber ($T < 250$ °C). The quench rate is inferred to be 500 °C/s, similar to that reported by Holloway et al. (1992) for a rapid-quench furnace with an equivalent thermal profile. The rotating furnace design used in this study provides a significant degree of control on the thermal characteristics of the critical heating zone. The temperature along the length of the experimental capsules was measured using three iconel-sheathed, chrome–alumel thermocouples. Temperature differences between the distal thermocouples ranged from 1 to 16 °C, ±2 °C. The argon medium pressure

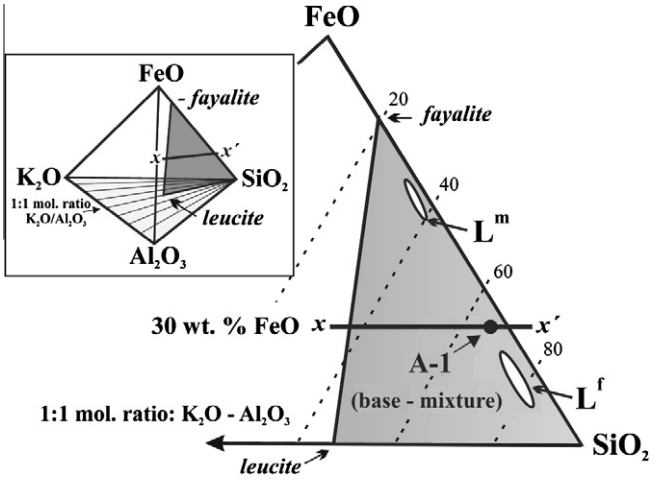

Fig. 1. Base-mixture composition A-1 plots on the 30 wt% isopleth (x–x') of the ternary join fayalite–leucite–silica. The join defines a composition plane bounded by the 1:1 molar ratio K_2O–Al_2O_3 segment in the system SiO_2–FeO–Al_2O_3–K_2O (inset). Experimental compositions comprise base-mixture A-1 with: H_2O, $H_2O + P$, or $H_2O + S$. Ellipses comprise the composition fields of experimental immiscible melts, (L^m) Fe-rich and (L^f) Si-rich, projected onto the volatile-free ternary join.

Table 1
Starting compositions for experimental melts (wt%). H_2O, P and S values are wt% total wt. oxides; P and S comprise 6.66×10^{-4} mol/g of total weight oxides.

Sample	SiO_2	FeO_{total}	Al_2O_3	K_2O	H_2O	P	S
A-1	60.05	27.27	1.87	1.72	9.09	–	–
AP-1	59.50	27.03	1.86	1.70	9.01	2.06	–
AS-1	58.97	26.79	1.89	1.69	8.93	–	2.14

was measured using a Bourdon tube-gauge, accurate to ±5 MPa.

Reversal experiments were performed to determine the time required to achieve chemical equilibrium in the experimental charges. Capsules containing experimental base-compositions +10 wt% H_2O, were heated for two hours at a temperature of 1210 °C and then cooled to 1075, 1150 or 1200 °C for 1, 2 or 4 h, and subsequently quenched. The chemical compositions and textural characteristics observed in the experimental products produced in the reverse experiments are identical to those produced in forward experiments run at the same temperature (Lester, 2012) and it is therefore concluded that equilibrium was obtained at heating durations of less than 1 h. Solid-oxide buffer reactants were evaluated after cooling using X-ray powder diffraction analysis or microscopic phase identification.

A part of the experimental product was mounted in epoxy and polished. Major element compositions of conjugate immiscible phases were analyzed with a Cameca SX-100 electron microprobe at the University of Manitoba. Analytical conditions were set to an accelerating voltage of 15 kV, 15 nÅ beam current, with a beam diameter of 5–10 μm for silicate and Fe-rich glasses. Material for stable oxygen isotope analysis was prepared by magnetic separation of finely-ground quench products under suspension in ethanol. The process was repeated (7–12 repititions) until it yielded samples containing over 95% of the desired conjugate glass were produced (determined by visual analysis of back-scatterer X-ray images). Oxygen isotope analyses were carried out using the BrF_5 procedure of Clayton and Mayeda (1963). Three to five milligrams of sample was analyzed and the estimated uncertainty in the isotope analyses is ±0.2‰ (std. dev., 2σ). All values are reported in the δ notation ($\delta^{18}O = \{[(^{18}O/^{16}O)\ \text{sample}/(^{18}O/^{16}O)\ \text{standard} - 1] * 1000\}$) in units of permil relative to VSMOW.

3. RESULTS

Six of the experiments produced immiscible Si-rich felsic silicate and Fe-rich mafic silicate (L^f and L^m) conjugate liquids (Fig. 2) from which the phases could be separated.

Differences in the $\delta^{18}O$ values of the conjugate liquids in the two-liquid field range from permil at 1100 °C, and from 0 to 0.4‰ at 1200 °C (Table 2). The Si-rich liquid is more ^{18}O-rich, as is expected given the correlation between ^{18}O enrichment and the concentration of network-forming components that has been documented for silicate minerals (Taylor and Epstein, 1962).

Composition AS-1, run at $fO_2 = MH$, $T = 1200$ °C, produced three liquids, an Si-rich liquid, an Fe-rich liquid and an Fe–S–O liquid. The differences in the $\delta^{18}O$ values of the conjugate Si- and Fe-rich liquids in equilibrium with the Fe–S–O liquid is 0.2‰, but in contrast to all other experiments, the Fe-rich liquid is more ^{18}O rich.

4. DISCUSSION

The addition of H_2O alone and H_2O with either P or S, to the systems Fe_2SiO_4–Fe_3O_4–$KAlSi_2O_6$–SiO_2, Fe_2SiO_4–Fe_3O_4–Fe_2O_3–$KAlSi_2O_6$–SiO_2, and Fe_3O_4–Fe_2O_3–$KAlSi_2O_6$–SiO_2 widens the two-liquid immiscibility field at temperatures between 1075 and 1200 °C, producing conjugate liquids with strongly divergent compositions (Watson, 1976; Visser and Koster van Groos, 1979; Lester, 2012). In this study, Fe-rich liquids (L^m) contain 42–61 wt% more FeO_{total} and 340–58 wt% less SiO_2 than conjugate Si-rich liquids (L^f) (Table 2).

In comparison, conjugate melts in the anhydrous system Fe_2SiO_4–$KAlSi_2O_6$–SiO_2 at 1180 °C differ by only 16–17 wt% FeO and 17–24 wt% SiO_2 (Kyser et al., 1998). If ^{18}O partitioning between the immiscible liquids is controlled by the relative abundance of tetrahedral Si–O and Al–O bonds in the two melts, as suggested by experimentally and theoretically determined fractionation factors for mineral pairs by O'Neil (1986) and Kyser (1987), then $\Delta^{18}O$ ($\delta^{18}O\ L^f - \delta^{18}O\ L^m$) values for the more compositionally diverse melts generated through the addition of H_2O with or without, P or S should be greater than those reported for the anhydrous system. However, the $\Delta^{18}O$ values of the volatile-rich conjugate melts pairs synthesized herein do not differ significantly from those of the anhydrous system. The $\Delta^{18}O$ values for melts with or without H_2O are nearly identical, ranging from 0.4–0.6‰, regardless of experimental fO_2 (Fig. 3).

No oxygen isotope fractionation data between immiscible melts in the systems Fe_3O_4–Fe_2O_3–$KAlSi_2O_6$–SiO_2 + P or S have been reported, so a comparison of $\Delta^{18}O$ values in melts with or without H_2O in combination with P and S cannot be made. To test the relationship between oxygen isotope fractionation and differences in the degree of melt polymerization produced by varying melt composition and fO_2, we use the parameter $(NBO/T^m)/(NBO/T^f)$, where NBO = number of non-bridging oxygens in the melt, T: tetrahedrally-coordinated network-forming cations; L^f: the felsic–silicate melt and L^m: the mafic silicate melt (Bogaerts and Schmidt, 2006), to describe the partitioning of oxygen bound in tetrahedral coordination between the conjugate melts.

Oxygen isotope proportioning as a function of the ratio of NBO/T (L^m) to NBOT (L^f) in the conjugate melts (Fig. 4) indicates no correlation between $\Delta^{18}O$ values and the partitioning of tetrahedral oxygen between conjugate melts in the anhydrous experiments, or in experiments with H_2O, or H_2O + S (Fig. 2). In contrast, the $\Delta^{18}O$ values of glasses with H_2O + P record a negative correlation with NBO/T (L^m) to NBO/T (L^f)/NBO/T (L^m). Melts in the H_2O-bearing experiments are in equilibrium with a vapor

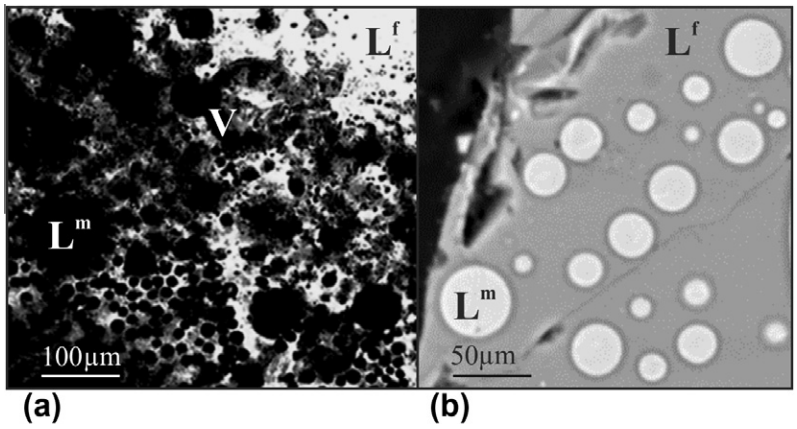

Fig. 2. (a and b) Experimental product, immiscible phases L^m (Fe-rich melt), L^f (Si-rich melt), and V (vapor). Images: (a) transmitted light, (b) back-scattered X-ray.

Table 2
Major element compositions and $\delta^{18}O$ values for conjugate immiscible glasses in the systems Fe_2SiO_4–Fe_3O_4–$KAlSi_2O_6$–SiO_2, Fe_3O_4–$KAlSi_2O_6$–SiO_2 and Fe_3O_4–Fe_2O_3–$KAlSi_2O_6$–SiO_2S or P, $P = 200$ MPa. Chemical compositions represent an average of nine electron microprobe analyses of conjugate Fe-rich (L^m) and Si-rich (L^f) glasses.

Sample	Temperature (°C)	fO_2		SiO_2	FeO	Al_2O_3	K_2O	P	S	$\delta^{18}O$	$\Delta^{18}O$ $\delta^{18}O$ L^f – $\delta^{18}O$ L^m
A-1	1100	QFM	L^f	84.66	6.43	2.90	2.57			13.8	0.5
			L^m	40.84	51.28	1.30	1.21	0.05		13.3	
AP-1	1100	NNO	L^f	66.05	17.86	7.61	5.57	0.54		12.5	0.8
			L^m	29.8	54.32	3.66	2.04	1.79		11.7	
AS-1	1100	NNO	L^f	88.38	7.94	2.43	1.72		0.1	12.7	0.4
			L^m	25.61	68.26	1.06	0.97		3.42	12.3	
A-1	1200	NNO	L^f	79.42	11.59	2.71	2.03			12.5	0.4
			L^m	40.05	55.69	1.91	0.76			12.1	
AP-1	1200	MH	L^f	82.06	6.79	4.32	4.22	0.36		18.6	0.3
			L^m	26.47	57.39	1.83	0.74	1.45		18.3	
AP-1	1200	QFM	L^f	84.66	6.43	2.90	2.57	0.01		13.4	0
			L^m	40.84	51.28	3.30	1.20	0.05		13.4	
AS-1	1200	MH	L^f	78.74	9.23	4.70	3.81		0.09	12.2	−0.2
			L^m	33.49	55.28	1.62	1.47		3.12	12.4	

phase and are considered to be saturated with respect to H_2O.

The depolymerizing effects of such high concentrations of H_2O in the experimental melts are not considered in the calculation of NBO/T here. However, even if the Si–Al network structure in the melts were strongly depolymerized by the inclusion of H_2O, as has been demonstrated in some hydrous silicate melts (e.g. $NaAlSi_3O_8$–H_2O: Mysen, 1991), the $\Delta^{18}O$ values of conjugate liquids should correlate with the partitioning of SiO_2 or FeO_{total}. No such correlation is observed in the melts produced here.

The temperature dependence of oxygen isotope fractionation between the conjugate melts is small over the experimental range of 1100–1200 °C. However, the $\Delta^{18}O$ values for all compositions with H_2O, and $H_2O + P$ at 1100 °C are slightly greater than those recorded at 1200 °C (Fig. 1). The trend is consistent with the negative temperature dependence of isotopic fractionation in melt–mineral and mineral–mineral pairs of similar compositions (e.g., Clayton and Kieffer, 1991; Zhao and Zheng, 2003), although the magnitude of the fractionation is much smaller for the melt–melt systems in this study.

Variation in the $\Delta^{18}O$ values of the melts as a function of fO_2 can be isolated in the systems Fa–Mt–Lc–Qtz + H_2O + P and Mt–Hm–Lc–Qtz + H_2O + P at 1200 °C, $\Delta^{18}O$ values are slightly higher at the more oxidizing conditions, showing an increase of 0.3‰ at MH over QFM. Variations in fO_2 could affect oxygen isotope proportioning in silicate melts by influencing the nature and distribution of oxygen-cation bonds between the conjugate melts, e.g. the concentrations of, and partitioning between, melts of Fe_2SiO_4, Fe_3O_4 and Fe_2O_3 (Kress and Carmichael, 1991) and S^{-2} and SO_4^- (Carroll and Webster, 1994; Moretti and Ottonello, 2005). However, the effect observed in the H_2O + P- bearing systems is not significant over the fO_2 range of the experiments (QFM–MH).

Comparison of theoretically-proposed $\Delta^{18}O$ values at 1100 and 1200 °C for andesite–magnetite, rhyolite–magnetite and quartz–magnetite pairs (Fig. 1) show that ^{18}O partitions preferentially into the Si-rich phase but $\Delta^{18}O$ values

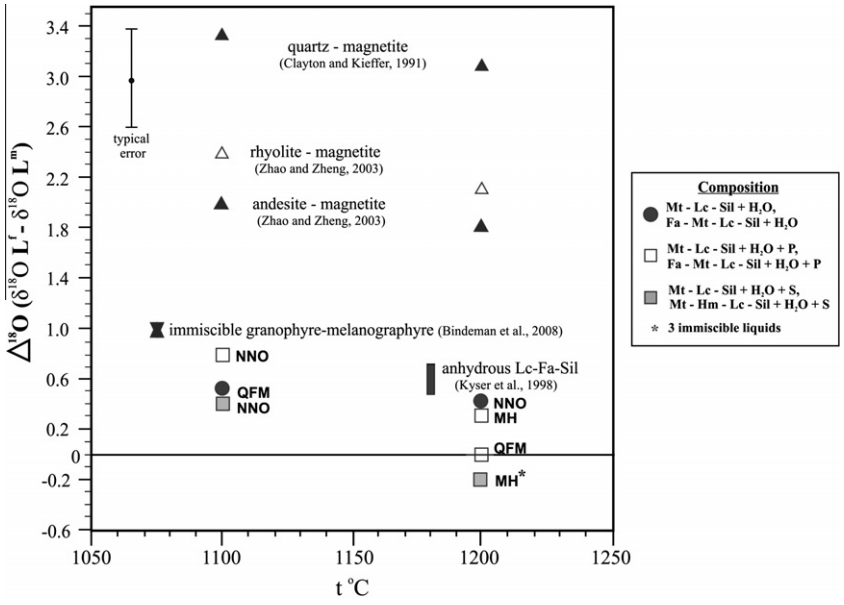

Fig. 3. $\Delta^{18}O$ between coexisting Si- and Fe-rich glasses, melt–mineral pairs and mineral–mineral pairs at temperatures of 1100, 1180, and 1200 °C. The pressures are 200 MPa for the experiments in this study and 0.1 MPa for Kyser et al. (1998). $\Delta^{18}O$ values between melt–mineral pairs, mineral–mineral pairs, and granophyre–melanogranophyre (Bindeman et al., 2008) are theoretical.

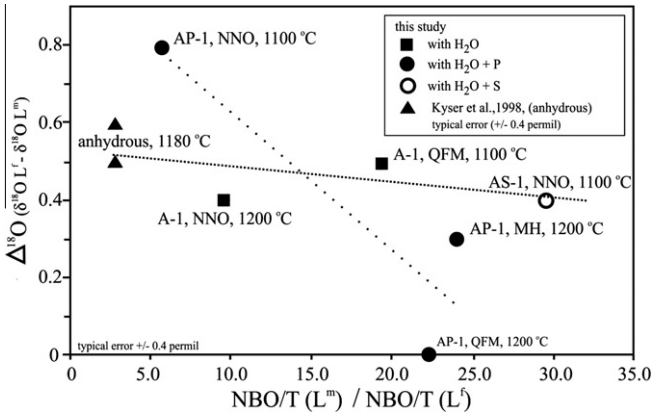

Fig. 4. Oxygen isotope proportioning as a function of tetrahedral oxygen partitioning in conjugate immiscible Si- and Fe-rich glasses at temperatures of 1100, 1180, and 1200 °C, $P = 200$ MPa and 0.1 MPa (Kyser et al., 1998). Disparity in the degree of melt polymerization between conjugate–liquid pairs increases from left to right.

for the melt–mineral and mineral–mineral pairs are significantly higher than those observed for the immiscible melts. Although the compositional range of the melt–mineral and mineral–mineral pairs is broadly analogous to the melt compositions in the present study (Clayton and Kieffer, 1991; Zhao and Zheng, 2003) their theoretical $\Delta^{18}O$ values are not good proxies for immiscible silicate melts.

5. CONCLUDING REMARKS

Liquid-phase separation in silicate melts with H_2O and $H_2O + P$ or S is attended by variations in the distribution of oxygen isotopes in conjugate melts. Thus the $\delta^{18}O$ values of the silicate-rich liquid are not significantly higher (0–0.8 ± 0.4‰) than those of the Fe-rich liquid. Although the preferential fractionation of ^{18}O into the silicate melts is consistent with crystallochemical effects on oxygen isotope distribution trend determined for mineral–mineral and melt–minerals pairs, the variation in ^{18}O ratios in immiscible melts does not correlate with variations in the distribution of Si–O and Al–O networks between the immiscible melts examined here. No systematic change occurs in oxygen isotope proportioning in the conjugate melts as the result of varying fO_2 over the range QFM–MH. The upper limit of the range of $\Delta^{18}O$ values (<1‰), and the variation in the $\delta^{18}O$ values of conjugate melts that occurs with the inclusion of network modifying constituents, suggest that in some cases, oxygen isotope ratios might be useful

to distinguish lithologies evolved from coexisting immiscible silicate melts, from lithologies that have evolved by crystal fractionation only.

REFERENCES

Bindeman I. N., Brooks C. K., McBirney A. R. and Taylor H. P. (2008) The low-$\delta^{18}O$ late-stage ferrodiorite magmas in the Skaergaard Intrusion: Result of liquid immiscibility, thermal metamorphism, or meteoric water incorporation into magma? *J. Geol.* **116**, 571–586.

Bogaerts M. and Schmidt M. W. (2006) Experiments on silicate immiscibility in the system Fe_2SiO_4–$KAlSi_3O_8$–SiO_2–CaO–MgO–TiO_2–P_2O_5. *Contrib. Miner. Petrol.* **152**, 257–274.

Carroll M. R. and Webster J. D. (1994) Solubilities of sulfur, noble gases, nitrogen, chlorine, and fluorine in magmas. In *Volatiles in Magmas, Reviews in Mineralogy*, vol. 30 (eds. M. R. Carroll and J. R. Holloway). Mineralogical Society of America, pp. 231–279.

Chou M. and Cygan G. L. (1990) Quantitative redox control and measurement in hydrothermal experiments. In *Fluid–Mineral Interactions: A Tribute to H. P. Eugster: Geochemical Society Special Publication* (eds. R. J. Spencer and I.-M. Chou) **2**, pp. 3–15.

Clayton R. N. and Kieffer S. W. (1991) Oxygen isotopic thermometer calibrations: In stable isotope geochemistry: A tribute to Samuel Epstein. *Geochem. Soc. Spec. Publ.* **3**, 3–10.

Clayton R. N. and Mayeda T. K. (1963) The use of bromine pentafluoride in the extraction of oxygen from oxides and silicates for isotopic analysis. *Geochim. Cosmochim. Acta* **27**, 43–52.

Holloway J. R. (1971) Internally heated pressure vessels. In *Research Techniques for High Temperature and Pressure* (eds. G. C. Ulmer and H. E. Barnes). Springer-Verlag, New York, pp. 217–257.

Holloway J. R., Dixon J. E. and Pawley A. R. (1992) An internally heated, rapid-quench, high-pressure vessel. *Am. Miner.* **77**, 643–646.

Kress V. C. and Carmichael I. S. E. (1991) The compressibility of silicate liquids containing Fe_2O_3 and the effect of composition, temperature, oxygen fugacity and pressure on their redox states. *Contrib. Miner. Petrol.* **108**, 82–92.

Kyser T. K. (1987) Equilibrium fractionation factors for stable isotopes. In *Short Course in Stable Isotope Geo-chemistry of Low Temperature Fluids*, vol. 13 (ed. T. K. Kyser). Mineralogical Association of Canada, pp. 1–84.

Kyser T. K. (1990) Stable isotopes in the continental lithospheric mantle. In *The Continental Lithospheric Mantle* (ed. M. Menzies). Oxford University Press, NY, pp. 127–156.

Kyser T. K., Lesher C. E. and Walker D. (1998) The effects of liquid immiscibility and thermal diffusion on oxygen isotopes in silicate liquids. *Contrib. Miner. Petrol.* **3**, 373–381.

Lester G. W. (2012) An experimental study of liquid-phase separation in the systems Fe_2SiO_4–Fe_3O_4–$KAlSi_2O_6$–SiO_2–H_2O, Fe_3O_4–$KAlSi_2O_6$–SiO_2–H_2O and Fe_3O_4–Fe_2O_3–$KAlSi_2O_6$–SiO_2–H_2O with or without P, S, F, Cl or $Ca_{0.5}$ $Na_{0.5}$ $Al_{1.5}$ $Si_{2.5}O_8$: Implications for immiscibility in volatile-rich natural magamas. Ph. D. dissertation, Queen's Univ., 2012-04-10 15:06:35.797, 95p.

Moretti R. and Ottonello G. (2005) Solubility and speciation of sulfur in silicate melts: The conjugated Toop-Samis-Flood-Grjotheim (CTSFG) model. *Geochim. Cosmochim. Acta* **69**, 801–823.

Mysen B. O. (1991) Relation between structure, redox equlibria of iron, and properties of magmatic liquids. *Adv. Phys. Chem.* **9**, 41–98.

O'Neil J. R. (1986) Theoretical and experimental aspects of isotope fractionations. In *Stable Isotopes in High Temperature Geological Processes, Reviews in Mineralogy*, vol. 16 (eds. J. W. Valley, H. P. Taylor and J. R. O'Neil). Mineralogical Society of America, Washington, DC, pp. 1–37.

Philpotts A. R. (2008) Comments on: Liquid immiscibility and the evolution of basaltic magma. *J. Petrol.* **49**(12), 2171–2175.

Pineau F., Javoy M. and Bottinga Y. (1976) $^{13}C/^{12}C$ ratios of rocks and inclusions in popping rocks of the Mid-Atlantic ridge and their bearing on the problem of deep-seated carbon. *Earth Planet. Sci. Lett.* **29**, 413–421.

Schuessler J. A., Roman R. E., Botcharnikov E., Behrens H., Misiti V. and Freda C. (2008) Oxidation state of iron in hydrous phono-tephritic melts. *Am. Miner.* **93**, 1493–1504.

Taylor H. P. and Epstein S. (1962) Relationship between $^{18}O/^{16}O$ ratios in coexisting minerals of igneous and metamorphic rocks part I. *Geol. Soc. Am. Bull.* **73**, 461–480.

Taylor H. P. and Sheppard S. M. F. (1986) Igneous rocks. I. Processes of isotopic fractionation and isotope systematic. In *Stable Isotopes in High Temperature Geological Processes. Reviews in Mineralogy*, vol. 16 (eds. J. W. Valley, H. P. Taylor and J. R. O'Neil). Mineralogical Society of America, pp. 227–272.

Veksler I. V., Dorfman A. M., Danyushevsky L. V., Jakobsen J. K. and Dingwell D. B. (2006) Immiscible silicate liquid partition coefficients: Implications for crystal-melt element partitioning and basalt petrogenesis. *Contrib. Miner. Petrol.* **152**, 685–702.

Vicenzi E., Green T. and Sie S. (1994) Effect of oxygen fugacity on trace-element partitioning between immiscible silicate melts at atmospheric pressure: A proton and electron microprobe study. *Chem. Geol.* **117**, 355–360.

Visser W. and Koster van Groos A. F. (1979) Effect of P_2O_5 and TiO_2 on liquid–liquid equilibria in the system K_2O–FeO–Al_2O_3–SiO_2. *Am. J. Sci.* **279**, 970–988.

Watson E. B. (1976) Two-liquid partition coefficients: Experimental data and geochemical implications. *Contrib. Miner. Petrol.* **56**, 119–134.

Zhao Z. F. and Zheng Y. F. (2003) Calculation of oxygen isotope fractionation in magmatic rocks. *Chem. Geol.* **193**, 59–80.

Associate editor: Edward M. Ripley